Table IX. Measured Infrared Frequencies (cm^{-1}) of Diazomethane and Iron–Diazomethane Complex in Solid Nitrogen

vibrational mode		$Fe(CH_2N_2)$	$Fe(^{13}CH_2N_2)$	$Fe(CHDN_2)$	$Fe(CD_2N_2)$
CH_2, CD_2[a]	A	427.2	419.0	390.3	337.7
CHD	B	784.4		797.3	
wag		831.4	825.0		
C=N, ^{13}C=N	A	1406.6	1397.4	1303.4	1211.6
stretch	B	1385.1	1377.2	1247.0	1050.0
CH_2, CD_2	A	3068.4	3063.6	2327.9	2236.8
s stretch	B	2900.7	2893.9		
CHD		2906.7	2899.0		
CD stretch					
CH_2, CD_2	A	3181.0	3169.2	3130.6	2407.9
a stretch	B	2966.0	2956.0	2948.0	
CHD		2972.0	2963.0		
CH stretch		2977.0	2967.0		

[a] A = CH_2N_2, B = $Fe(CH_2N_2)$.

matrices are listed in Table VII.

Finally, iron atoms react spontaneously with diazomethane in nitrogen matrices to yield a set of frequencies thought to arise from $(N_2)_xFeCH_2$ species. Although the N≡N stretching region is complicated by $Fe_2(N_2)_x$ bands, the absence of absorptions in the 1800-cm^{-1} region indicates that no "side-on" $(N_2)_xFeCH_2$ species are formed.

A selected region of the infrared spectrum of $(N_2)_xFeCH_2$ is presented in Figure 7 along with $FeCH_2$ and N_2FeCH_2 in an argon matrix. The frequencies of $(N_2)_xFeCH_2$ and the isotopically labeled species are tabulated in Table VIII.

$Fe(CH_2N_2)$ complexes, better described as $(N_2)_xFe(CH_2N_2)$, were also found in nitrogen matrices. They lead to $(N_2)_xFeCH_2$ species after $\lambda \geq 500$ nm photolysis. The absorption frequencies of these species are presented in Table IX.

The iron/diazomethane reactions in cryogenic matrices can be summarized as shown in Scheme I.

Finally, we have demonstrated that ternary reactions can be investigated readily using matrix isolation spectroscopy, suggesting that a large number of fundamental organometallic processes can be investigated using the technique.

Acknowledgment. We gratefully acknowledge The Robert A. Welch Foundation and the 3M Co. for support of this work.

Registry No. CH_3FeH, 83615-51-4; $(N_2)CH_3FeH$, 115912-13-5; $^{13}CH_3FeH$, 115912-24-8; $(N_2)^{13}CH_3FeH$, 115912-14-6; CH_2DFeD, 115912-25-9; $(N_2)CH_2DFeD$, 115912-15-7; CD_2HFeH, 115912-26-0; $(N_2)CD_2HFeH$, 115912-16-8; CD_3FeD, 115912-27-1; $(N_2)CD_3FeD$, 115912-17-9; Fe, 7439-89-6; CH_4, 74-82-8; H_2, 1333-74-0; $^{13}CH_4$, 6532-48-5; $Fe^{13}CH_2$, 115912-28-2; N_2FeCH_2, 115912-18-0; $FeCH_2$, 95250-85-4; D_2, 7782-39-0; $FeCD_2$, 115912-29-3; N_2FeCD_2, 115941-34-9; CH_3FeOH, 115912-30-6; CH_2DFeOD, 115912-31-7; CD_3FeOD, 115912-32-8; $N_2Fe^{13}CH_2$, 115912-19-1; N_2FeCHD, 115912-20-4; FeCHD, 115941-35-0; CH_2N_2, 334-88-3; HFeCH, 115912-21-5; $HFe^{13}CH$, 115912-22-6; DFeCD, 115912-23-7.

Association of Dimethyl Sulfide Radical Cation with Dimethyl Sulfide. Strength of a Two-Center Three-Electron Bond

A. J. Illies,* P. Livant, and M. L. McKee

Contribution from the Department of Chemistry, Auburn University, Auburn, Alabama 36849-5312. *Received March 31, 1988*

Abstract: A mass spectrometer designed to study gas-phase ion–molecule association equilibria was used to measure $\Delta G°$ for the reaction of $(CH_3)_2S$ (**1**) with $(CH_3)_2S^+$ (**2**) to give $[(CH_3)_2S–S(CH_3)_2]^+$ (**3**). The sulfur–sulfur bond in **3** is an example of a two-center three-electron (2c 3e) bond. From the measured $\Delta G°$ of −13.4 kcal/mol at 252 °C a bond strength ($\Delta H°$) of −23.9 to −26.5 kcal/mol was estimated, assuming a $\Delta S°$ of −20 to −25 cal/mol·K. In addition, a study of other ion–molecule reactions occurring in the **1** + **2** system was performed. Ab initio calculations were performed on **1**–**3** at the [PMP2/6-31G*]//3-21G(*) level, on SF_2, SF_2^+, and $[F_2S–SF_2]^+$ at the [PMP2/6-31G*]//3-21G(*) level, and on H_2S, H_2S^+, and $[H_2S–SH_2]^+$ at the PMP4SDTQ/6-31G*//3-21G(*) + zero-point correction level. The latter calculation gave $\Delta H° = -26.2$ kcal/mol for $H_2S + H_2S^+ \rightarrow [H_2S–SH_2]^+$. A $\Delta H°$ of −27.4 kcal/mol for **1** + **2** → **3** was calculated. This value of $\Delta H°$ was modified by including corrections taken from the higher level $H_2S + H_2S^+$ calculation to give $\Delta H° = -25.5$ kcal/mol, which agrees with the values derived from the experiment. In the $SF_2 + SF_2^+ \rightarrow [F_2S–SF_2]^+$ system a $\Delta H°$ of −12.2 kcal/mol was calculated.

Two-center three-electron (2c 3e) bonds have been the subject of considerable recent experimental and theoretical interest, especially 2c 3e sulfur–sulfur bonds.[1] Clark[2] has very recently published a theoretical description of odd-electron σ bonds and provided an extensive survey of the literature, which will not be repeated here. The focus in the present paper is on 2c 3e sulfur–sulfur bonding, exclusively. The 2c 3e sulfur–sulfur bond that would appear to be "simplest" is that produced by bonding of H_2S to the H_2S radical cation. However, the possibility (see below) that the $[H_2S---SH_2]^+$ "dimer" may be bound by a proton (viz. $[H–S–H---SH_2]^+$) instead of by a S–S 3e bond makes it desirable to study an example free of such complications. The simplest example is shown in eq 1, the reaction of dimethyl sulfide radical cation (**2**) with dimethyl sulfide (**1**).

$$\underset{\mathbf{1}}{(CH_3)_2S} + \underset{\mathbf{2}}{(CH_3)_2S^+} \rightleftarrows \underset{\mathbf{3}}{[(CH_3)_2S---S(CH_3)_2]^+} \quad (1)$$

Reaction 1 is a prototype for the formation of the dimeric radical cations observed by ESR for a variety of sulfides, **4**,[3] and

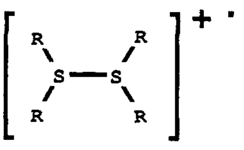

4

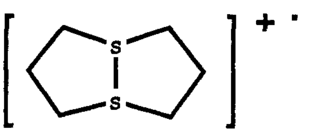

5

---

(1) (a) Asmus, K.-D. *Acc. Chem. Res.* **1979**, *12*, 436. (b) Glass, R. S.; Hojjatie, M.; Petsom, A.; Wilson, G. S.; Göbl, M.; Mahling, S.; Asmus, K.-D. *Phosphorus Sulfur* **1985**, *23*, 143–168. (c) For a recent paper with many leading references, see: Drewello, T.; Lebrilla, C. B.; Schwarz, H.; deKoning, L. J.; Fokkens, R. H.; Nibbering, N. M. M.; Anklam, E.; Asmus, K.-D. *J. Chem. Soc., Chem. Commun.* **1987**, 1381–1383.

(2) Clark, T. *J. Am. Chem. Soc.* **1988**, *110*, 1672–1678.

0002-7863/88/1510-7980$01.50/0

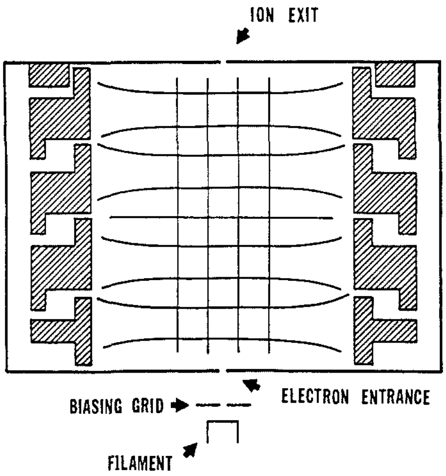

Figure 1. Schematic of ion source. Shaded areas represent overlapping drift guard rings. Equipotential lines are indicated in the center of the ion source region.

for the formation of the transannular S–S 2c 3e bond in medium rings such as 1,5-dithiacyclooctane (**5**).[4] While much effort has gone into the detection of species with 2c 3e bonds, very little is known about the strength of such bonds, especially for organic examples. The question has been explored theoretically, but no data of an unambiguous nature exist with which to judge the quality of the calculations.

The dissociation energies of several ionic gas-phase clusters that might conceivably involve 2c 3e S–S bonds have been measured: $[CS_2–S_2]^+$ (21.9[5] and 28.4 kcal/mol[6]), $[CS_2–S]^+$ (39.7 kcal/mol[7]), $[CS_2–CS]^+$ (36.0 kcal/mol[6]), $[CS_2–CS_2]^+$ (21.9,[5] 17.5,[8] 18.2,[8] and 11.3 kcal/mol[9]). In each case, however, the mode of bonding is a matter of speculation; thus, these dissociation energies may or may not refer to 2c 3e S–S bonds. The work described herein on the dissociation of **3** is the first gas-phase study of a 2c 3e S–S bond free from any ambiguity.

Experimental Section

The work reported here was carried out on a highly modified Du Pont 491B mass spectrometer, which has been recently described in detail elsewhere.[10] A few aspects of the experiments pertinent to this work will be presented here. The ion source has coaxial ionizing electron entrance and ion exit apertures, shown schematically in Figure 1. The ion drift distance through the source is 2.00 cm. Because of the geometry, nascent ions are formed by electron impact in a region of the source that is aligned with the ion exit slit and hence the entrance to the mass spectrometer. Overlapping drift guard rings shape the electric fields in the source. Ions drift through the gas at a constant velocity due to the controlled potential gradient and the relatively high pressures (which result in many collisions as the ions travel through the source). Time-resolved experiments are possible by pulsing a biasing grid between the filament and the electron entrance (Figure 1).

The coaxial arrangement of the ionizing electron beam and ion exit apertures and the controlled electric fields result in high ion sensitivities at low-ionizing electron energies. Because of the high ion sensitivity, it is possible to study ion–molecule reactions of primary ions formed at low energies uncomplicated by reactions of fragment ions, which are produced at higher energies. When the energy is varied, it is sometimes possible to identify ion–molecule reactions originating from fragment ions. This situation can be contrasted with conventional high-pressure ion sources where the ionizing electron beam is perpendicular to the ion exit slit.[11-13] With those sources, in order for electron penetration into the region of the source from which ion sampling takes place, it is necessary to use high electron energies, typically 100–2000 eV.[11,12] Since high electron energies are required to produce a sufficient number of ions for detection, both primary and fragment ions are almost always present.

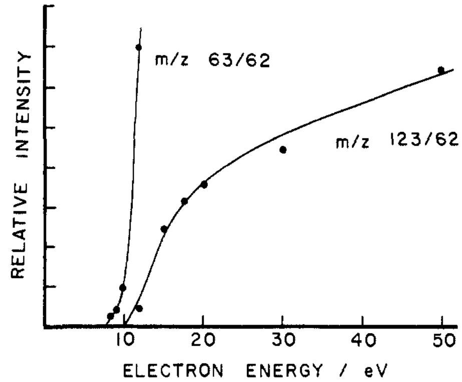

Figure 2. Intensities of *m/z* 63 and 123, normalized to the intensity of *m/z* 62, as a function of ionization energy. Total pressure was 0.44 Torr. Concentration of dimethyl sulfide in krypton was 1.5%.

Aldrich gold-label dimethyl sulfide was dried by condensing it twice in sequence onto 3-Å molecular sieves, which had been baked overnight at 250 °C (10^{-4} Torr). The total ion source pressure was typically 0.50 Torr with dimethyl sulfide concentrations less than 3% and average ion residence times of approximately 500 μs. In order to avoid pressure-dependent differential diffusion effects through inlet leak valves, dilutions with krypton or CF_4 were accomplished by mixing the gases in the inlet system itself rather than introducing gas mixtures. The pressure in the ion source was measured with an MKS capacitance manometer. Mass spectra were recorded by conventional analog recording techniques while residence time distributions were collected by techniques previously described.[10]

Calculations were performed using the GAUSSIAN 86 program package[14] and standard basis sets.[15]

Results and Discussion

Ion–Molecule Reactions. At low pressures, in the limit of no collisions, ion–molecule reactions do not take place, and therefore one expects to observe (at the appropriate electron energies) predominantly parent and fragmentation ions. We found that, at low pressures of dimethyl sulfide with no bath gas present, with the solid sample reentrant open, and at electron energies near threshold, only *m/z* 62, corresponding to the parent ion, **2**, was observed. As the ionizing electron energy was increased, *m/z* 47 and 61 were also observed and correspond to the fragmentation processes in eq 2 and 3. The abundances of these ions change in a manner consistent with the reported ionization and appearance potentials of 9.28, 11.08, and 11.5 eV for *m/z* 62 (**2**), 47 (**4**), and 61 (**5**), respectively.[16] Collisional activation mass spectral studies

$$\underset{\mathbf{2}}{(CH_3)_2S^+} \rightarrow \underset{\mathbf{4}\ (m/z\ 47)}{CH_2{=}SH^+} + CH_3 \qquad (2)$$

$$\underset{\mathbf{2}}{(CH_3)_2S^+} \rightarrow \underset{\mathbf{5}\ (m/z\ 61)}{[CH_3S{=}CH_2]^+} + H \qquad (3)$$

---

(3) (a) Qin, X.-Z.; Meng, Q.-C.; Williams, F. *J. Am. Chem. Soc.* **1987**, *109*, 6778–6788. (b) Wang, J. T.; Williams, F. *J. Chem. Soc., Chem. Commun.* **1981**, 1184. (c) Wang, J. T.; Williams, F. *Ibid.* **1983**, 980. (d) Rao, D. N. R.; Symons, M. C. R.; Wren, B. W. *J. Chem. Soc., Perkin Trans. 2* **1984**, 1681. (e) Gilbert, B. G.; Hodgeman, D. K. C.; Norman, R. O. C. *Ibid.* **1973**, 1748. (f) Izuoka, A.; Kobayashi, M. *Chem. Lett.* **1981**, 1603–1604. (g) Petersen, R. L.; Nelson, D. J.; Symons, M. C. R. *J. Chem. Soc., Perkin Trans 2* **1978**, 225.

(4) Musker, W. K. *Acc. Chem. Res.* **1980**, *13*, 200–206.

(5) Meot-Ner, M.; Field, F. H. *J. Chem. Phys.* **1977**, *66*, 4527.

(6) Ono, Y.; Linn, S. H.; Prest, H. F.; Gress, M. E.; Ng, C. Y. *J. Chem. Phys.* **1981**, *74*, 1125.

(7) Gress, M. E.; Linn, S. H.; Ono, Y.; Prest, H. F.; Ng, C. Y. *J. Chem. Phys.* **1980**, *72*, 4242.

(8) Ono, Y.; Linn, S. H.; Prest, H. F.; Gress, M. E.; Ng, C. Y. *J. Chem. Phys.* **1980**, *73*, 2523.

(9) Trott, W. M.; Blais, N. C.; Walters, E. A. *J. Chem. Phys.* **1979**, *71*, 1692.

(10) Illies, A. J. *J. Phys. Chem.* **1988**, *92*, 2889.

(11) Sharma, D. K.; deHojer, S. M.; Kebarle, P. *J. Am. Chem. Soc.* **1985**, *107*, 3757.

(12) Meot-Ner, M. *J. Am. Chem. Soc.* **1987**, *109*, 7947.

(13) Hiraoka, K.; Takimoto, H.; Yamabe, S. *J. Am. Chem. Soc.* **1987**, *109*, 7346.

(14) Frisch, M. J.; Binkley, J. S.; Schlegel, H. B.; Raghavachari, K.; Melins, C. F.; Martin, R. L.; Stewart, J. J. P.; Bobrowicz, F. W.; Rohlfing, C. M.; Kahn, L. R.; Defrees, D. J.; Seeger, R.; Whiteside, R. A.; Fox, D. J.; Fleuder, E. M.; Pople, J. A. *GAUSSIAN 86*; Carnegie-Mellon Quantum Chemistry Publishing Unit, Carnegie-Mellon University: Pittsburgh, PA, **1984**.

(15) For a description of basis sets, see: Hehre, W. J.; Radom, L.; Schleyer, P. v. R.; Pople, J. A. *Ab Initio Molecular Orbital Theory*; Wiley: New York, 1986.

have shown **4** to be protonated thioformaldehyde rather than CH_3S^+.[17]

At higher pressures (0.007 Torr for dimethyl sulfide with krypton added to a total pressure of 0.44 Torr), namely in the pressure range in which ion-molecule collisions and hence reactions occur, the situation can be more complex. At very low ionizing energies, only *m*/*z* 62 (**2**) and 124 (**3**) are observed. As the electron energy is raised only slightly *m*/*z* 63 and 123 appear. The peaks at *m*/*z* 47 and 61 are essentially absent at the high pressures. The results of a study of ion abundances as a function of ionizing energy are shown in Figure 2. The intensities for *m*/*z* 63 and 123 are normalized to the *m*/*z* 62 intensity. The data strongly suggest that *m*/*z* 63 and 123 have different precursors. We postulate *m*/*z* 63 to arise as shown in eq 4 and *m*/*z* 123 to arise as shown in eq 5. The fact that at low pressures (nearly

$$\underset{\mathbf{4}\ (m/z\ 47)}{CH_2{=}SH^+} + \underset{\mathbf{1}}{(CH_3)_2S} \rightarrow CH_2{=}S + \underset{\mathbf{7}\ (m/z\ 63)}{(CH_3)_2SH^+} \qquad (4)$$

$$\underset{\mathbf{5}\ (m/z\ 61)}{[CH_3S{=}CH_2]^+} + \mathbf{1} \rightarrow \underset{\mathbf{8}\ (m/z\ 123)}{[CH_3SCH_2S(CH_3)_2]^+} \qquad (5)$$

collision free conditions) *m*/*z* 47 and at high pressure *m*/*z* 63 have lower appearance potentials than *m*/*z* 61 and 123, respectively, is again consistent with the literature appearance potentials for **4** and **5**. The behavior of *m*/*z* 63 as a function of ionization energy is inconsistent with its arising from protonation by adventitious H_3O^+, hence, *m*/*z* 63 must arise from hydrogen abstraction or proton transfer by a fragment. Proton transfer is what is depicted in eq 4. We have drawn **8** with a C–S bond in eq 5 because MNDO calculations carried out by us indicate that this form is lower in energy than an alternative S–S bonded structure, $[(CH_3)(CH_2{=})S{\cdots}S(CH_3)_2]^+$.

The above-described studies involved ion abundances as a function of electron energy for processes that occur near the ionization threshold. As the ionizing energy is raised still further, many new peaks appear in the mass spectrum. Möckel[18] has reported the conventional CI mass spectrum of **1** as *m*/*z* 61 (2.4), 62 (19.3), 63 (100), 123 (5.9), 124 (18.7), and 125 (1.7) with methane ionization gas. These data are generally consistent with our experience at higher pressure. We made no attempt to sort out the reaction details for all the high energy reactions. These experiments led to the practical conclusion that, to avoid the complications caused by the intrusion of the reactions shown in eq 2–5, equilibrium reaction 1 should be studied at low ionization energies. Accordingly, all studies of reaction 1 were carried out with ionization energies less than 8.5 eV (nominal). At this ionization energy, *m*/*z* 62 (**2**) and *m*/*z* 124 (**3**) are present to the virtual exclusion of all other ions.

Equilibrium Studies. The equilibrium reaction of eq 1 was studied with ionization voltages near threshold in Kr bath gas. In order for the intensities measured for **2** and **3** to be validly used to calculate an equilibrium constant for eq 1, it must be demonstrated convincingly that the system in the ion source chamber is at equilibrium. In this study, three criteria were applied: (1) The residence time distribution for *m*/*z* 62 must be the same as the residence time distribution for *m*/*z* 124.[10,19] (2) The measured equilibrium constant (K_{app}) must be independent of extraction voltage (which is applied to move ions out of the ion source and hence is related to the average residence time of ions in the source).[10] (3) K_{app} must be independent of the total pressure in the source (P_t). The average drift properties of ions in equilibrium are the same since the charge that is detected undergoes many switching reactions. This results in identical residence time distributions for ions in equilibrium and forms the basis for the first criterion. Figure 3 shows residence time distributions that are clearly superimposable. Thus, the first criterion is met. Plots of K_{app} versus extraction voltage were always linear with slopes of essentially zero. Thus, criterion 2 is met. We found however that K_{app} varied with P_t under a variety of conditions, including various temperatures, various concentrations of **1** in Kr, and a different bath gas, CF_4. Some curves of ln K_{app} versus P_t are shown in Figure 4. At low pressures (typically below 0.4 Torr) there are simply too few collisions for equilibrium to be attained. Residence time distributions for **2** and **3** were not superimposable in this region, indicating that equilibrium has not been attained in the ion source chamber, and ln K_{app} increases with increasing P_t. At higher pressures (0.7–1.4 Torr typically) ln K_{app} falls as P_t is increased, yet residence time distributions for **2** and **3** were superimposable. A possible explanation of the high-pressure drop-off of ln K_{app} is that collision-induced dissociation of **3** occurs just outside the exit aperture of the ion source chamber, which would cause K_{app} to be too low. However, when the region outside the ion source chamber was flooded with Kr, K_{app} did not change, ruling out this possible explanation for the high-pressure drop-off of K_{app}. Figure 4 shows ln K_{app} versus P_t for several concentrations of **1** in CF_4 at 525 K. (Since the partial pressure of **1** is held constant and P_t is varied by changing the partial pressure of CF_4, the concentration of **1** varies in one run.) In general, lower concentrations of **1** reach their peak ln K_{app} at higher P_t and exhibit less of a drop-off in ln K_{app} than higher concentrations of **1**. Curves similar to those shown in Figure 4 obtained at lower temperatures show a more pronounced high-pressure drop-off at all concentrations. We consider the data shown in Figure 4 for **1** (0.0074 Torr) to demonstrate the linearity expected for a well-behaved system, i.e. one that meets all three criteria for equilibrium.

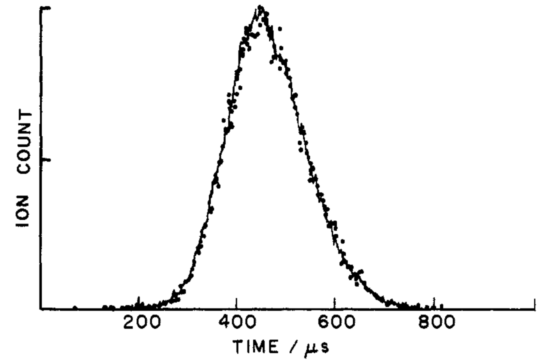

Figure 3. Distribution of residence times of various ions in the ion source chamber: points, *m*/*z* 62; solid line, *m*/*z* 124.

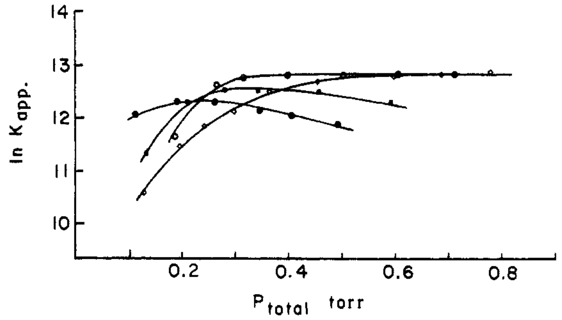

Figure 4. Apparent equilibrium constant as a function of total pressure in the reaction chamber. Pressure of the bath gas (CF_4) was varied while the pressure of dimethyl sulfide remained constant. Dimethyl sulfide pressures were as follows: (◇) 0.0050, (○) 0.0074, (■) 0.0150, (●) 0.0383 Torr.

These data lead to $\Delta G_{525}° = -13.4$ kcal/mol. On the basis of examination of an extensive compilation of thermodynamic data for gas-phase ion-molecule associations,[20] a reasonable estimate for $\Delta S°$ is −20 to −25 eu. This corresponds to $\Delta H°$ of −23.9 to

---

(16) Rosenstock, H. M.; Draxl, K.; Steiner, B. W.; Herron, J. T. *J. Phys. Chem. Ref. Data* **1977**, *6*(1).

(17) (a) McLafferty, F. W.; Dill, J. D. *J. Am. Chem. Soc.* **1978**, *100*, 2907. (b) McLafferty, F. W.; Dill, J. D. *Ibid.* **1979**, *101*, 6526. (c) Pope, S. A.; Hillier, I. H.; Guest, M. F. *Chem. Phys. Lett.* **1984**, *104*, 191. (d) Nobes, R. H.; Bouma, W. J.; Radom, L. *J. Am. Chem. Soc.* **1984**, *106*, 2774.

(18) Möckel, H. J. *Fresenius' Z. Anal. Chem.* **1979**, *295*, 241–247.

(19) Chang, C.; Sroka, C. J.; Meisels, G. G. *J. Chem. Phys.* **1971**, *55*, 5154.

(20) Keesee, R. G.; Castleman, A. W., Jr. *J. Phys. Chem. Ref. Data* **1986**, *15*, 1011–1071.

Table I. Total Energies (Hartrees), Bond Energy, ΔS, Zero-Point Energies, Geometries, and Vibrational Frequencies for H_2S, H_2S^+, and $(H_2S)_2{}^+$

	H_2S	H_2S^+	$(H_2S)_2{}^+$	ΔH^a	ΔH^b
HF/3-21G(*)	−396.819 637	−396.476 389	−793.332 709	−23.02	−19.79
HF/6-31G	−398.626 687	−398.276 611	−796.933 536	−18.98	−15.75
MP2/6-31G	−398.684 283	−398.321 956	−797.048 878	−24.88	−21.65
PMP2/6-31G		−398.322 854	−797.050 910	−27.48	−24.25
HF/6-31G*	−398.667 322	−398.326 990	−797.026 070	−19.93	−16.70
MP2/6-31G*	−398.788 224	−398.425 352	−797.261 010	−29.77	−26.54
PMP2/6-31G*		−398.427 227	−797.264 009	−30.48	−27.25
MP3/6-31G*	−398.806 532	−398.444 218	−797.296 792	−28.90	−25.67
PMP3/6-316G*		−398.445 212	−797.298 230	−29.18	−25.95
MP4SDQ/6-31G*	−398.809 492	−398.448 002	−797.302 918	−28.51	−25.28
PMP4SDQ/6-31G*[c]		−398.448 996	−797.304 356	−28.79	−25.56
MP4SDTQ/6-31G*	−398.811 622	−398.449 496	−797.308 054	−29.46	−26.23
PMP4SDTQ/6-31G*[c]		−398.450 490	−797.309 492	−29.74	−26.51
ZPE, kcal/mol	10.28	10.07	23.94		
ΔS, eu	49.0	50.4	70.3		
geometry (3-21G(*))	S–H 1.327 H–S–H 94.2	S–H 1.335 H–S–H 95.4	S–S 2.837 S–H 1.328 H–S–H 94.9 tilt[d] 91.6		
vibr freq, cm^{-1} (3-21G(*))	1381 2903 2906	1362 2840 2842	69 249[e] 457 477 554 604 1372 1379 2893 2896 2900 2900		

[a] In kcal/mol, for $H_2S + H_2S^+ \rightarrow (H_2S)_2{}^+$. [b] In kcal/mol including zero-point energy correction, for $H_2S + H_2S^+ \rightarrow (H_2S)_2{}^+$. Zero-point correction is multiplied by a factor of 0.9. [c] Correction for spin contamination taken from the PMP3/6-31G* calculation. [d] Angle between the S–S bond form the bisector of the H–S–H angle. Lines bisecting both H–S–H angles from a dihedral angle of 180°. [e] S–S stretch.

−26.5 kcal/mol for the reaction in eq 1. Since ΔH° is in this case probably nearly equivalent to the bond energy (neglecting the heat capacity differences of the reactants and products), this range is currently the best available experimental value of the bond strength of a 2c 3e sulfur–sulfur bond.[21] We are presently attempting to modify our apparatus so that higher temperatures are accessible.

At the temperatures at which these experiments were done (150–250 °C), no peaks above m/z 124 could be seen. However, when the reaction chamber was cooled to −40 °C, a very prominent peak at m/z 182 was observed. This corresponds to a monopositive trimer of dimethyl sulfide *less four amu*. The structure of this species is a tantalizing mystery.

Calculations. High-level ab initio calculations were carried out on the species involved in reaction 1 as well as the analogous reaction of F_2S with F_2S^+ to give $[F_2S\text{–}SF_2]^+$ and the reaction of H_2S with H_2S^+ to give $[H_2S\text{–}SH_2]^+$. This latter reaction has been treated theoretically by Clark[2,22] and Fernandez et al.[23] Our calculations on the $H_2S + H_2S^+$ system were performed at increasingly more refined levels of theory (see Table I) and culminated in a PMP4SDTQ/6-31G*//3-21G(*) + zero-point correction calculation (the "P" indicating that the effect of the largest spin contaminant was projected out of the correlation energies for open-shell systems), which gave $\Delta H^\circ = -26.5$ kcal/mol. The 2c 3e S–S bond stretching frequency is predicted to be 224 cm^{-1} (the value listed in Table I multiplied by a factor of 0.9),[24] with a calculated bond length of 2.797 Å. The calculated vibrational frequencies lead to an estimate of ΔS° of −29.1 eu. Clark[2] has previously calculated a ΔH° for this system of −27.7 kcal/mol at the MP2/6-31G* level. Our work shows that the correction for zero-point energies (3.23 kcal/mol) is a significant fraction of the calculated bond energy.

Table II. Total Energies (Hartrees), Bond Energy, and Geometries for $(CH_3)_2S$, $(CH_3)_2S^+$, and $((CH_3)_2S)_2{}^+$

	$(CH_3)_2S$	$(CH_3)_2S^+$	$((CH_3)_2S)_2{}^+$	ΔH^a
HF/3-21G(*)	−474.456 985	−474.174 441	−948.663 185	−19.94
HF/6-31G	−476.666 185	−476.377 378	−953.068 990	−15.96
HF/6-31G*	−476.735 306	−476.454 582	−953.215 341	−15.98
MP2/6-31G	−476.905 332	−476.599 676	−953.547 670	−26.78
PMP/6-31G		−476.600 841	−953.549 792	−27.38
[PMP2/ 6-31G*]				−27.40
geometry (3-21G(*))	C–S 1.813 C–S–C 99.4	C–S 1.795 C–S–C 102.9	C–S 1.808 S–S 2.797 C–S–C 101.1 tilt[b] 99.4	

[a] In kcal/mol, for $(CH_3)_2S + (CH_3)_2S^+ \rightarrow ((CH_3)_2S)_2{}^+$. [b] Angle between the S–S bond and the line bisecting the C–S–C angle. The lines bisecting the C–S–C angles form a dihedral angle of 180°.

Fernandez et al.[23] carried out a series of calculations on H_2S, H_2S^+, $(H_2S)_2$, and $(H_2S)_2{}^+$ aimed at explaining the results of photoionization experiments[25] on the $(H_2S)_2$ system, which resulted in a bond energy of −21.2 kcal/mol for the $(H_2S)_2{}^+$ ion. The

---

(21) While equilibrium constants for formation of systems similar to **3** have been measured in aqueous media (Bonifacic, M.; Asmus, K. D. *J. Chem. Soc., Perkin Trans. 2* **1980**, 758, and references therein), it is of importance to obtain thermodynamic data by using systems free of the complications of solvent and counterion, as has been done here.

(22) (a) Clark, T. *J. Comput. Chem.* **1981**, *2*, 261–265. (b) Clark, T. *NATO Adv. Study Inst., Ser. C* **1986**, *189*, 49.

(23) Fernandez, P. F.; Ortiz, J. V.; Walters, E. A. *J. Chem. Phys.* **1986**, *84*, 1653–1658.

(24) Pople, J. A.; Schlegel, H. B.; Krishnan, R.; DeFrees, D. J.; Binkley, J. S.; Frisch, M. J.; Whiteside, R. A.; Hout, R. F.; Hehre, W. J. *Int. J. Quantum Chem., Symp.* **1981**, *15*, 269.

(25) (a) Blais, N. C.; Walters, E. A. *J. Chem. Phys.* **1981**, *75*, 4208. (b) Blais, N. C.; Walters, E. A. *Ibid.* **1984**, *80*, 3501. (c) Prest, H. F.; Tzeng, W. B.; Brom, J. M., Jr.; Ng, C. Y. *J. Am. Chem. Soc.* **1983**, *105*, 7531.

Table III. Total Energies (Hartrees), Bond Energy, and Geometries for SF_2, SF_2^+, and $(SF_2)_2^+$

	SF_2	SF_2^+	$(SF_2)_2^+$	ΔH^a
3-21G(*)	−593.418870	−593.074529	−1186.508443	−9.44
6-31G	−596.200809	−595.791094	−1191.997781	−3.69
6-31G*	−596.312151	−595.971582	−1192.296798	−8.20
PMP2/6-31G	−596.502353	−596.100232	−1192.618321	−9.88
[PMP2/ 6-31G*]				−14.39
geometry (3-21G(*))	S–F 1.592 F–S–F 98.3	S–F 1.516 F–S–F 100.5	S–F 1.551 S–S 2.866 F–S–F 99.4 tilt^b 88.1	

^{a} In kcal/mol, for $SF_2 + SF_2^+ \rightarrow (SF_2)_2^+$. ^{b} Angle between the S–S bond and the line bisecting the F–S–F angle. The lines bisecting the F–S–F angles form a dihedral angle of 180°.

calculations indicated that the $(H_2S)_2^+$ dimer is more appropriately described as H_3S^+ bound by electrostatic forces to an SH radical. Therefore, the structures of the neutral van der Waals molecule, $(H_2S)_2$, and of the dimer ion, $(H_2S)_2^+$, might not pertain to a 2c 3e bond. Our calculations and those of Clark on the $H_2S + H_2S^+$ system should be viewed as didactic exercises designed to illuminate the nature of the 2c 3e S–S bond in a computationally simple system rather than calculations aimed at explaining experimental results, which, as Fernandez et al. point out, may not be measuring the strength of a $[H_2S\text{-}\text{-}\text{-}SH_2]^+$ sulfur–sulfur bond. (There is evidence, nonetheless, for the existence of $[H_2S\text{-}\text{-}\text{-}SH_2]^+$ in aqueous solution.)[26]

On the other hand, it is difficult to envision the $(CH_3)_2S + (CH_3)_2S^+$ system involving anything other than a 2c 3e S–S bond. Therefore, our calculations on this system may be compared directly and unambiguously to our experimental data. At the [PMP2/6-31G*]//3-21G(*) level (brackets indicate that the additivity approximation[27] was used), a $\Delta H°$ of −27.4 kcal/mol is calculated (see Table II). This value may be improved in an approximate way by applying the zero-point correction from the H_2S system, as well as the correction found in the H_2S system on going from [PMP2] to the full PMP4 level. The $\Delta H°$ obtained in this way is −25.5 kcal/mol, which is in excellent agreement with the range of values derived from the experimental measurements.

In order to explore substituent effects on 2c 3e bond energy, the $SF_2 + SF_2^+$ system was calculated (see Table III). At the [PMP2/6-31G*]//3-21G(*) level a $\Delta H°$ of −14.4 kcal/mol was found. When we applied the same "corrections" here as were applied in the $(CH_3)_2S + (CH_3)_2S^+$ case, the $\Delta H°$ obtained is −12.2 kcal/mol, which is about half the bond energy calculated for the non-fluorine-containing cases.

Note Added in Proof: Gill and Radom have recently reported the same theoretical binding energy for $(H_2S)_2^+$, namely 26.5 kcal/mol.[28]

Acknowledgment. M.L.M. thanks the donors of the Petroleum Research Fund, administered by the American Chemical Society, for partial financial support.

---

[26] Chaudhri, S. A.; Asmus, K.-D. *Angew. Chem., Int. Ed. Engl.* **1981**, *20*, 672–673.

[27] (a) McKee, M. L.; Lipscomb, W. N. *J. Am. Chem. Soc.* **1981**, *103*, 4673. (b) Nobes, R. H.; Bouma, W. J.; Radom, L. *Chem. Phys. Lett.* **1982**, *89*, 497. (c) McKee, M. L.; Lipscomb, W. N. *Inorg. Chem.* **1985**, *24*, 762.

[28] Gill, P. M. W.; Radom, L. *J. Am. Chem. Soc.* **1988**, *110*, 4931–4941.

Unstable Enols in the Gas Phase. Preparation, Ionization Energies, and Heats of Formation of (*E*)- and (*Z*)-2-Buten-2-ol, 2-Methyl-1-propen-1-ol, and 3-Methyl-2-buten-2-ol

František Tureček,*,† Libor Brabec,‡ and Jorma Korvola*,§

Contribution from Baker Laboratory, Department of Chemistry, Cornell University, Ithaca, New York 14853-1301, The J. Heyrovsky Institute of Physical Chemistry and Electrochemistry, Czechoslovak Academy of Sciences, Prague, Czechoslovakia, and the Department of Chemistry, University of Jyväskylä, Kyllikinkatu 1-3, SF-40100 Jyväskylä, Finland. Received April 20, 1988

Abstract: (*E*)-2-Buten-2-ol (**1**), (*Z*)-2-buten-2-ol (**2**), 2-methyl-1-propen-1-ol (**3**), and 3-methyl-2-buten-2-ol (**4**) were prepared as transient species by flash-vacuum pyrolysis of the corresponding methylated bicyclo[2.2.1]hept-5-en-2-ols and characterized by mass spectrometry. Threshold ionization energies (IE) were determined as IE(**1**) = 8.42 ± 0.04, IE(**2**) = 8.44 ± 0.03, IE(**3**) = 8.44 ± 0.03, and IE(**4**) = 8.15 ± 0.04 eV. Cation radical $[\mathbf{4}]^{\bullet+}$ was generated from 3,3-dimethyl-2-hexanone, and its appearance energy and heat of formation were determined as AE = 9.33 ± 0.09 eV and $\Delta H_f° = 545 \pm 10$ kJ·mol^{-1}. The heats of formation of the neutral enols **1**–**4** were determined as −212, −214, −207, and −241 kJ·mol^{-1}, respectively. The experimental heats of formation are compared with those predicted from Benson's additivity rules or calculated by the semiempirical MNDO method. Substituent effects on the heats of formation, proton affinities, and relative thermochemical and kinetic stabilities of simple enols are discussed.

Simple enols[1] appear as transient intermediates in a variety of fundamental organic reactions, namely aldol condensation,[2] electrophilic substitution in carbonyl compounds,[3] oxy-Cope,[4] Conia,[5] and Caroll rearrangements,[6] and others.[7] In view of the key role enols play in the kinetics of several organic reactions, there is demand for thermodynamic data that would allow the quan-

---

[†] Cornell University.

[‡] Czechoslovak Academy of Sciences.

[§] University of Jyväskylä.

[1] Hart, H. *Chem. Rev.* **1979**, *79*, 515.

[2] House, H. O. *Modern Synthetic Reactions*, 2nd ed.; Benjamin: Menlo Park, 1972; Chapter 10, pp 629–733.

[3] (a) Toullec, J.; El-Alaoui, M. *J. Org. Chem.* **1986**, *51*, 4054. (b) Toullec, J. *Adv. Phys. Org. Chem.* **1982**, *18*, 1.